CISM International Centre for Mechanical Sciences 603
Courses and Lectures

Basilio Lenzo *Editor*

Vehicle Dynamics

Fundamentals and Ultimate Trends

International Centre
for Mechanical Sciences

Springer

CISM International Centre for Mechanical Sciences

Courses and Lectures

Volume 603

For more than 40 years the book series edited by CISM, “International Centre for Mechanical Sciences: Courses and Lectures”, has presented groundbreaking developments in mechanics and computational engineering methods. It covers such fields as solid and fluid mechanics, mechanics of materials, micro- and nanomechanics, biomechanics, and mechatronics. The papers are written by international authorities in the field. The books are at graduate level but may include some introductory material.

More information about this series at https://link.springer.com/bookseries/76

Basilio Lenzo
Editor

Vehicle Dynamics

Fundamentals and Ultimate Trends

Springer

Editor
Basilio Lenzo
University of Padova
Padua, Italy

ISSN 0254-1971 ISSN 2309-3706 (electronic)
CISM International Centre for Mechanical Sciences
ISBN 978-3-030-75882-0 ISBN 978-3-030-75884-4 (eBook)
https://doi.org/10.1007/978-3-030-75884-4

This Springer imprint is published by the registered company Springer Nature Switzerland AG
The registered company address is: Gewerbestrasse 11, 6330 Cham, Switzerland

Preface

Since the invention of the world's first motor vehicle, more than 100 years ago, automobiles have been widely accepted in our society with the progress of modern industry. The study and understanding of vehicle dynamics have always played a crucial role in the design of vehicles, with the aim of guaranteeing safety and stability as well as good performance. The recent advent of electric vehicles and the future perspective of widespread autonomous cars have posed further interesting challenges for the vehicle dynamicist. Nonetheless, the importance of the basics should never be underestimated—after all, essentially a vehicle behaviour is described by second Newton's law, $F = ma$.

With these motivations, an international course was organised at CISM in 2019, with a team of lecturers including two eminent academics, two experienced researchers, and two industrial representatives. The aim of this book—which collects contributions from the lecturers—is to recall the fundamentals of vehicle dynamics and to present and discuss the state of the art of ultimate trends in the field, including torque vectoring control, vehicle state estimation, and autonomous driving.

The first chapter, "Fundamentals on Vehicle and Tyre Modelling", discusses the equations of motion for a generic vehicle, including roll and pitch dynamics as well as the vertical travel of the sprung mass. Then, the chapter deals with the fundamentals of tyre modelling, with a detailed analysis of the existing tyre models. Finally, a new linear tyre model with varying parameters is presented, which is at the same time simple—which makes it suitable for control purposes—and accurate in that it represents combined tyre-road interactions (longitudinal and lateral).

The second chapter, "Vehicle Steering and Suspension Kinematics/Compliance and Their Relationship to Vehicle Performance", is dedicated to the analysis of the key peculiarities of vehicle steering and suspension systems. After looking into tyre behaviour, the chapter dives into wheel end architecture and suspension kinematics, with the analysis of the suspension design parameters (camber, caster, kingpin, etc.) and their effects on vehicle behaviour, together with suspension compliance. Steering kinematics and compliance are discussed, along with the relationships between weight transfer, kinematics, and compliance. The final part deals with the interesting concept of tyre utilisation.

In the third chapter, "Tyre Mechanics and Thermal Effects on Tyre Behaviour", the structure of the tyre and the mechanisms involved in tyre-road interaction are analysed. The effect of temperature on the tyre behaviour is then examined. Detailed thermal models are presented, accounting for heat generation—due to both the tyre-road tangential interactions and the tyre cyclic deformation during rolling—and heat exchange at different levels. Finally, the chapter discusses the factors involved in tyre wear and the different approaches proposed so far to model it.

The second part of the book, devoted to ultimate trends in vehicle dynamics, begins with the chapter "Torque Vectoring Control for Enhancing Vehicle Safety and Energy Efficiency". The chapter first presents the principle of torque vectoring and the general framework of a torque vectoring system. Different approaches to define the vehicle reference yaw rate and reference sideslip angle are compared, with a focus on the design of the full vehicle cornering response and the definition of driving modes selectable by the driver. Various control methodologies and torque distribution strategies are discussed, along with their implications for vehicle safety and energy efficiency.

After introducing the motivations for the need of state estimators, the fifth chapter, "State and Parameter Estimation for Vehicle Dynamics", presents an accurate analysis of the principles of observers and estimators and the methods to implement them. The well-known Kalman filter is contextualised and presented with rigour, together with its variants. The important concept of observability is dealt with, including its physical interpretation and the support of enlightening examples. A specific estimation methodology is discussed in detail, able not only to estimate relevant vehicle states (such as the sideslip angle), but also tyre parameters.

The sixth chapter, "Automated Driving Vehicles", is dedicated to the future of vehicles: autonomous driving. After an introduction on the role of the driver, the chapter discusses the key aspects of sensor fusion, including typical sensor characteristics and requirements, and how to use them to obtain a reliable representation of the environment. Assuming the availability of such representation, the problem of motion planning is dealt with, resulting in the desired driving path and speed profile. Then, the chapter discusses control techniques for the vehicle to follow the desired path and to track the desired speed profile. Finally, verification, validation, and safety issues are addressed.

I would like to thank all the authors for their precious contributions. I trust this book will be a valid resource for graduate students and researchers in the field of vehicle dynamics and control.

Padua, Italy Basilio Lenzo

Contents

Fundamentals on Vehicle and Tyre Modelling

Moad Kissai

Abstract Many books provide vehicle dynamics and tire dynamics equations. Most of them are either too complex or too simplified for global Vehicle Motion Control (VMC). This chapter is focusing on the couplings that exist between longitudinal, lateral and vertical dynamics at both the vehicle and tire level. The equations provided are simple but sufficient for global VMC. Several research papers and industrial patents tend to provide a control strategy for a standalone system. Simplified car models are taken into consideration from the beginning. As we are steering towards global VMC, more complex models are needed. Here, we start from complex equations that are simplified enough to facilitate control synthesis while capturing the required couplings for a coordinated control. Results show how this simplified global dynamics equations are close enough to more complex high-fidelity models. These equations should be therefore used for the next generation of global VMC.

Car manufacturers and equipment suppliers are constantly proposing new attractive subsystems to stand out from their competitors. Recently, a large interest has been given particularly to automated vehicles. Automation promises indeed safer and smarter vehicles. Several researches have been carried out on one hand in robotic vision, sensor fusion, decision algorithms, big data management, and others. On the other hand, car manufacturers are looking closely on the over-actuation of the vehicle itself (Shyrokau & Wang, 2012; Soltani, 2014; Sriharsha, 2016). Indeed, giving the vehicle new features such as the ability of steering the rear wheels (Seongjin, 2015),

The original version of this chapter was revised: Figure 2 caption has been revised as follows "The sprung and unsprung masses decomposition (Modified from: Milliken W. & Milliken D. (1994) Race Car Vehicle Dynamics, p. 115. ©SAE International)". The correction to this chapter is available at https://doi.org/10.1007/978-3-030-75884-4_8

M. Kissai (✉)
Autonomous Systems and Robotics Lab, Department of Computer and System Engineering (U2IS), ENSTA Paris, Palaiseau, France
e-mail: moad.kissai@ensta-paris.fr

corrected publication 2022
B. Lenzo (ed.), *Vehicle Dynamics*, CISM International Centre for Mechanical Sciences 603, https://doi.org/10.1007/978-3-030-75884-4_1

distributing the brake torques or/and the engine torques differently between left and right tires (Siampis et al., 2013) and so on, can expand the vehicle's performance and generate new motion possibilities and car behaviors. This can be actually achieved provided that a global chassis control strategy can be designed.

The development of such strategies can be structured using the "V" development process. This approach is well-accepted for mechatronic systems development although it originates from system engineering and software development (Soltani, 2014). This method consists of feedback steps starting from requirement definition and ending up with in-vehicle validation. a Model Based Design (MBD) methodology is selected as it has proven its effectiveness along with the "V" development process in control system development (Nicolescu & Mosterman, 2010). Even if this approach may differ slightly according to the control architecture adopted, the main steps remain:

- System Modeling: Describing mathematically the physical representations of the system dynamics. This is a key step in an MBD design methodology due to the fact that the control logic developed is closely related to the model itself,
- Controllers Synthesis: Developing the different algorithms required to control the vehicle dynamics based on the system modeling,
- Coordination Strategy Development: as the overall system is over-actuated, coordination between subsystems should be ensured in order to satisfy the high-level demands.

In this chapter, we will mainly focus on the first step, namely, system modeling. More specifically, we will separate the dynamics of the vehicle only, and those of the tire, as it is the only effector of ground vehicles and deserves to be given a special attention.

1 Global Vehicle Modeling

Since today's passenger cars are more and more over-actuated, a bicycle model would probably not be any longer sufficient to describe vehicle dynamics. Here instead, a global four-wheeled vehicle model will be developed. We particularly put the spotlight on the internal couplings that may arise in case of simultaneous maneuvers, as braking when turning. These couplings may lead to interactions between subsystems, which may result in internal conflicts. For a proper construction of vehicle motion equations, we adopt the ISO 8855-2011 shown in Fig. 1.

In order to take into account the dynamic couplings, vertical load transfer, influence of suspensions and so on, the vehicle will be broken down into two supposedly undeformable masses: the **sprung mass**,[1] and the **unsprung mass**,[2] as Fig. 2 shows.

[1] Includes the vehicle body, engine, passengers and so on.

[2] Includes the wheels, suspensions, brakes and so on.

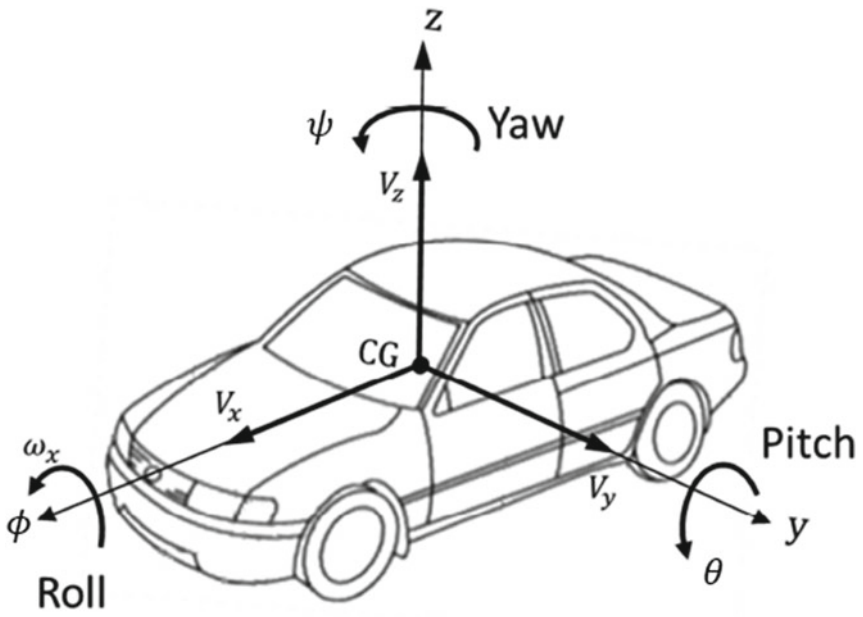

Fig. 1 Vehicle Axis System (ISO 8855-2011)

In addition, to take into account the differences between the influence of the front axle and the rear axle (especially for a 4 Wheel Steering (4WS) vehicle), the unsprung mass is also decomposed into two supposedly undeformable masses. We then have $\Sigma = S_s + S_{uf} + S_{ur}$, with:

- Σ: the overall vehicle of mass M and Center of Gravity (CoG) G,
- S_s: the sprung mass of mass M_s and CoG G_s,
- S_{uf}: the front unsprung mass of mass M_{uf} and CoG G_{uf},
- S_{ur}: the rear unsprung mass of mass M_{ur} and CoG G_{ur}.

1.1 Vehicle Dynamics

We define the dynamic torsor of the vehicle at the point G as follows:

$$\left\{\mathcal{D}\left(\Sigma/\mathcal{R}_g\right)\right\}_G = \left\{ \begin{array}{c} M\vec{\Gamma}\left(G/\mathcal{R}_g\right) \\ \vec{\delta}\left(G,\,\Sigma/\mathcal{R}_g\right) = \int_{\forall P\in\Sigma} \vec{GP} \wedge \vec{\Gamma}\left(P/\mathcal{R}_g\right) dm \end{array} \right\}_G \tag{1}$$

with:

- $\mathcal{R}_g$: the inertial frame of reference,

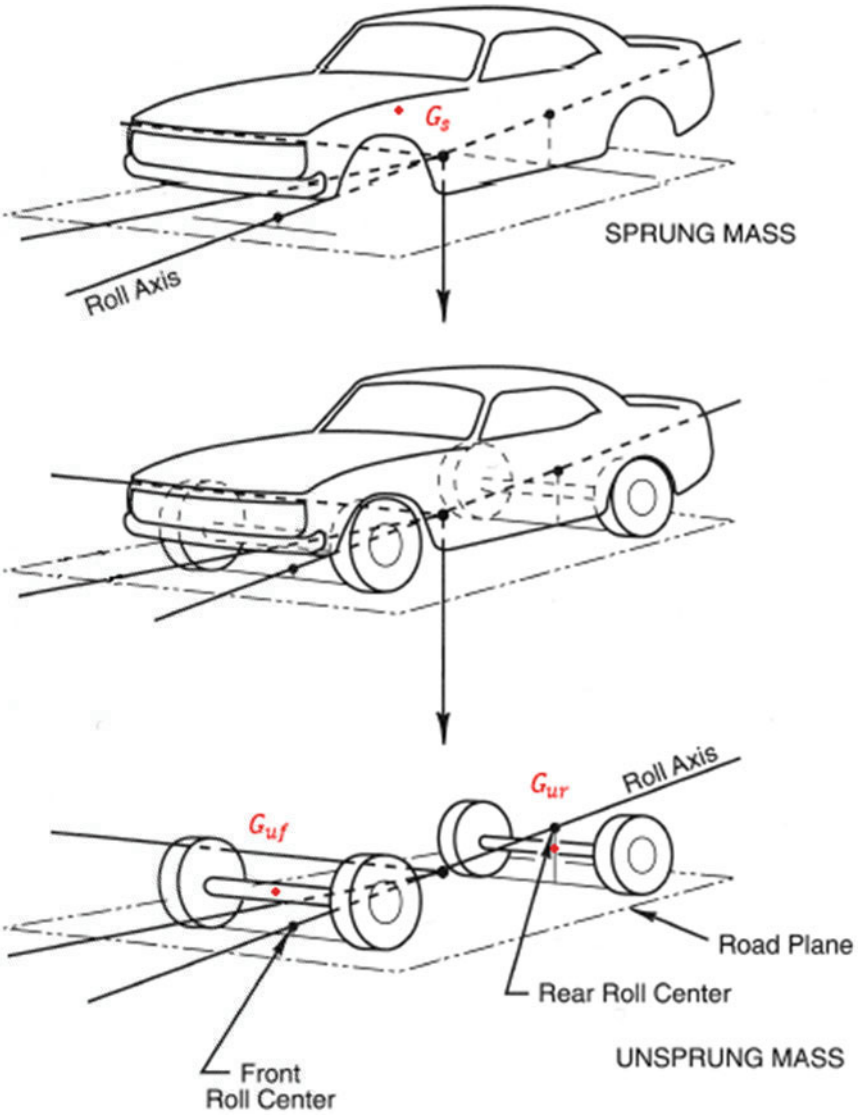

Fig. 2 The sprung and unsprung masses decomposition (Modified from: Milliken W. & Milliken D. (1994) Race Car Vehicle Dynamics, p. 115. ©SAE International)

- $\vec{\Gamma}$: the acceleration vector,
- $\vec{\delta}$: the dynamic moment.

We define also the exterior contact efforts as follows:

$$\left\{\mathcal{A}\left(\overline{\Sigma} \rightarrow \Sigma\right)\right\}_G = \left\{ \begin{array}{c} \vec{F}\left(\overline{\Sigma} \rightarrow \Sigma\right) \\ \vec{M}\left(G, \overline{\Sigma} \rightarrow \Sigma\right) \end{array} \right\}_G \tag{2}$$

with:

- $\overline{\Sigma}$: the complement of the system Σ,
- $\vec{F}$: the exterior efforts vector,
- $\vec{M}$: the exterior efforts moment vector.

The generalization of the fundamental law of dynamics is then (Pommier & Berthaud, 2010):

$$\left\{\mathcal{D}\left(\Sigma/\mathcal{R}_g\right)\right\}_G = \left\{\mathcal{A}\left(\overline{\Sigma} \rightarrow \Sigma\right)\right\}_G \tag{3}$$

This gives two fundamentals laws:

- The dynamic resultant theorem (linear motion):

$$M\vec{\Gamma}\left(G/\mathcal{R}_g\right) = \vec{F}\left(\overline{\Sigma} \rightarrow \Sigma\right) \tag{4}$$

- The dynamic moment theorem (angular motion):

$$\vec{\delta}\left(G, \Sigma/\mathcal{R}_g\right) = \vec{M}\left(G, \overline{\Sigma} \rightarrow \Sigma\right) \tag{5}$$

Moreover, the decomposition approach adopted allows us to partition the calculations using the torsor's properties:

$$\left\{\mathcal{D}\left(\Sigma/\mathcal{R}_g\right)\right\}_G = \left\{\mathcal{D}\left(S_s/\mathcal{R}_g\right)\right\}_G + \left\{\mathcal{D}\left(S_{uf}/\mathcal{R}_g\right)\right\}_G + \left\{\mathcal{D}\left(S_{ur}/\mathcal{R}_g\right)\right\}_G \tag{6}$$

1.2 Dynamic Torsor Calculation

1.2.1 Linear Equations of Motion

Because the CoG of the sprung mass can move with respect to the unsprung mass, it is simpler to first consider a fixed point to establish the equations of motion and then deduce the motion of the CoG (Noxon, 2012). Here, we consider the roll center that we note "O". The velocity at this point is noted:

$$\vec{V}\left(O/\mathcal{R}_g\right) = V_{O_x}\vec{i} + V_{O_y}\vec{j} \tag{7}$$

where $\vec{i}$ and $\vec{j}$ are the unit vectors of the chassis frame in the longitudinal and lateral direction respectively.

Because the chassis frame moves with respect to the inertial frame, and because the unsprung mass do not exhibit any roll nor pitch motions, we have:

$$\begin{aligned}\vec{\Gamma}\left(O/\mathcal{R}_g\right) &= \begin{vmatrix}\dot{V}_{O_x}\\ \dot{V}_{O_y}\\ 0\end{vmatrix} + \begin{vmatrix}0\\ 0\\ \dot{\psi}\end{vmatrix} \wedge \begin{vmatrix}V_{O_x}\\ V_{O_y}\\ 0\end{vmatrix} \\ &= \left(\dot{V}_{O_x} - \dot{\psi}V_{O_y}\right)\vec{i} + \left(\dot{V}_{O_y} + \dot{\psi}V_{O_x}\right)\vec{j}\end{aligned} \tag{8}$$

The same procedure can be applied to the points G_s, G_{uf} and G_{ur}. Regarding the front unsprung mass, we get:

$$\begin{aligned}\vec{V}\left(G_{uf}/\mathcal{R}_g\right) &= \begin{vmatrix}V_{O_x}\\ V_{O_y}\\ 0\end{vmatrix} + \begin{vmatrix}0\\ 0\\ \dot{\psi}\end{vmatrix} \wedge \begin{vmatrix}l_f\\ 0\\ h_f\end{vmatrix} \\ &= V_{O_x}\vec{i} + \left(\dot{V}_{O_y} + \dot{\psi}l_f\right)\vec{j}\end{aligned} \tag{9}$$

where h_f is the vertical distance between O and G_{uf}. Regarding the acceleration:

$$\begin{aligned}\vec{\Gamma}\left(G_{uf}/\mathcal{R}_g\right) &= \left.\frac{d\vec{V}\left(G_{uf}/\mathcal{R}_g\right)}{dt}\right|_{\mathcal{R}_g} \\ &= \vec{\Gamma}\left(O/\mathcal{R}_g\right) + \begin{vmatrix}0\\ 0\\ \ddot{\psi}\end{vmatrix} \wedge \begin{vmatrix}l_f\\ 0\\ h_f\end{vmatrix} + \begin{vmatrix}0\\ 0\\ \dot{\psi}\end{vmatrix} \wedge \left(\begin{vmatrix}0\\ 0\\ \dot{\psi}\end{vmatrix} \wedge \begin{vmatrix}l_f\\ 0\\ h_f\end{vmatrix}\right) \\ &= \left(\dot{V}_{O_x} - \dot{\psi}V_{O_y} - l_f\dot{\psi}^2\right)\vec{i} + \left(\dot{V}_{O_y} + \dot{\psi}V_{O_x} + l_f\ddot{\psi}\right)\vec{j}\end{aligned} \tag{10}$$

In the same way, we find for the rear unsprung mass:

$$\begin{cases}\vec{V}\left(G_{ur}/\mathcal{R}_g\right) = V_{O_x}\vec{i} + \left(V_{O_y} - \dot{\psi}l_r\right)\vec{j} \\ \vec{\Gamma}\left(G_{ur}/\mathcal{R}_g\right) = \left(\dot{V}_{O_x} - \dot{\psi}V_{O_y} + l_r\dot{\psi}^2\right)\vec{i} + \left(\dot{V}_{O_y} + \dot{\psi}V_{O_x} - l_r\ddot{\psi}\right)\vec{j}\end{cases} \tag{11}$$

Regarding the sprung mass, the equations are slightly more complicated as the vehicle's body turns with respect to the unsprung mass. Roll and pitch angles, noted respectively ϕ and θ, are introduced. The relationship between the vehicle's body frame and the chassis frame is:

$$\begin{pmatrix}\vec{i}_s\\ \vec{j}_s\\ \vec{k}_s\end{pmatrix} = \begin{pmatrix}\cos\theta & 0 & -\sin\theta\\ \sin\phi\sin\theta & \cos\phi & \sin\phi\cos\theta\\ \cos\phi\sin\theta & -\sin\phi & \cos\phi\cos\theta\end{pmatrix}\begin{pmatrix}\vec{i}\\ \vec{j}\\ \vec{k}\end{pmatrix} \tag{12}$$

We then obtain:

$$\vec{V}\left(G_s/\mathcal{R}_g\right) = \left| \begin{array}{c} V_{O_x} - \dot{\theta}\left(l_s \sin\theta + h_s \cos\phi\cos\theta\right) + \dot{\phi}h_s \sin\phi\sin\theta - \dot{\psi}h_s \sin\phi \\ V_{O_y} + \dot{\phi}h_s \cos\phi + \dot{\psi}\left(l_s \cos\theta - h_s \cos\phi\sin\theta\right) \\ \dot{\theta}\left(l_s \cos\theta - h_s \cos\phi\sin\theta\right) - \dot{\phi}h_s \sin\phi\cos\theta \end{array} \right. \tag{13}$$

where l_s and h_s are the horizontal and vertical distances between G_s and O respectively.

However, due to the transformation in Eq. (12), the acceleration equations obtained are very large to be exposed in this chapter. Nevertheless, we can propose at this point several simplifications. We suppose relatively small values of the roll and pitch angles and angular velocities with respect to yaw dynamics. This gives:

$$\left\{ \begin{array}{cccc} \sin\phi \approx \phi & \cos\phi \approx 1 & \sin\theta \approx \theta & \cos\theta \approx 1 \\ \phi\theta \approx 0 & \dot{\phi}\dot{\theta} \approx 0 & \dot{\phi}^2 \approx 0 & \dot{\theta}^2 \approx 0 \end{array} \right\} \tag{14}$$

In addition, to be able to apply the dynamic resultant theorem (4), we have to bring the calculation to a single point: G. To do so, we make use of the definition of the center of mass:

$$\vec{OG} = \frac{\sum_i m_i \vec{OG_i}}{\sum_i m_i} \tag{15}$$

Therefore, with the simplifications in (14):

$$\begin{aligned} M\vec{\Gamma}\left(G/\mathcal{R}_g\right) &= M_s\vec{\Gamma}\left(G_s/\mathcal{R}_g\right) + M_{uf}\vec{\Gamma}\left(G_{uf}/\mathcal{R}_g\right) + M_{ur}\vec{\Gamma}\left(G_{ur}/\mathcal{R}_g\right) \\ &= \left| \begin{array}{c} M\left(\dot{V}_{O_x} - \dot{\psi}V_{O_y}\right) - \ddot{\theta}M_s\left(l_s\theta + h_s\right) - \ddot{\psi}M_s h_s\phi + \dot{\psi}^2 M h_g\theta - 2\dot{\phi}\dot{\psi}M_s h_s \\ M\left(\dot{V}_{O_y} + \dot{\psi}V_{O_x}\right) + \ddot{\phi}M_s h_s - \ddot{\psi}M h_g\theta - \dot{\psi}^2 M_s h_s\phi - 2\dot{\theta}\dot{\psi}M_s\left(l_s\theta + h_s\right) \\ \ddot{\theta}M_s\left(l_s - h_s\theta\right) - \ddot{\phi}M_s h_s\phi \end{array} \right. \end{aligned} \tag{16}$$

where h_g is the horizontal distance between O and G.

1.2.2 Angular Equations of Motion

The dynamic moment, defined in any point A, is deduced from the "angular moment" noted σ using the definition (Pommier & Berthaud, 2010):

$$\vec{\delta}\left(A, S/\mathcal{R}_g\right) = \left.\frac{d\vec{\sigma}\left(A, S/\mathcal{R}_g\right)}{dt}\right|_{\mathcal{R}_g} + M\vec{V}\left(A/\mathcal{R}_g\right) \wedge \vec{V}\left(G/\mathcal{R}_g\right) \tag{17}$$

By choosing $A = G$, this definition is simplified:

$$\vec{\delta}\left(G, \Sigma/\mathcal{R}_g\right) = \left.\frac{d\vec{\sigma}\left(G, \Sigma/\mathcal{R}_g\right)}{dt}\right|_{\mathcal{R}_g} \tag{18}$$

Again, we first calculate the angular moment with respect to the reference point O and for each undeformable mass apart. The definition of the angular moment applied to the front unsprung mass is as follows (Pommier & Berthaud, 2010):

$$\vec{\sigma}\left(O, S_{uf}/\mathcal{R}_g\right) = M_{uf} O\vec{G}_{uf} \wedge \vec{V}\left(O/\mathcal{R}_g\right) + \overline{I_{uf}}\left(O, S_{uf}\right).\vec{\Omega}_c \tag{19}$$

where I_{uf} is the inertia tonsor of the mass S_{uf}. Its definition applied to any vector $\vec{u}$ at the point O is:

$$\overline{I_{uf}}\left(O, S_{uf}\right).\vec{u} = -\int_{P\in S_{uf}} \left[\vec{OP} \wedge \left(\vec{OP} \wedge \vec{u}\right)\right] dm \tag{20}$$

$\vec{\Omega}_c$ is the angular velocity vector, which, in this case, contains only the yaw rate.

Using the theorem of Huygens-Steiner (Pommier & Berthaud, 2010), we obtain:

$$\overline{I_{uf}}\left(O, S_{uf}\right) = \begin{pmatrix} I_{x_{uf}} + M_{uf}h_{uf}^2 & 0 & -I_{xz_{uf}} + M_{uf}l_f h_{uf} \\ 0 & I_{y_{uf}} + M_{uf}\left(l_f^2 + h_{uf}^2\right) & 0 \\ -I_{xz_{uf}} + M_{uf}l_f h_{uf} & 0 & I_{z_{uf}} + M_{uf}l_f^2 \end{pmatrix} \tag{21}$$

with $I_{x_{uf}}$, $I_{y_{uf}}$, and $I_{z_{uf}}$ are the inertia moment in the longitudinal, lateral, and vertical direction with respect to the point G_{uf} respectively. The zeros are due to the fact that S_{uf} is symmetric with respect to the plane $\left(G_{uf}, x, z\right)$. The additional terms are due to the theorem of Huygens-Steiner and the fact that the expressions have been brought to the point O. We finally get:

$$\vec{\sigma}\left(O, S_{uf}/\mathcal{R}_g\right) = \begin{vmatrix} M_{uf}h_{uf}\left(V_{O_y} + l_f\dot{\psi}\right) - I_{xzuf}\dot{\psi} \\ -M_{uf}h_{uf}V_{O_x} \\ M_{uf}l_f\left(V_{O_y} + l_f\dot{\psi}\right) + I_{zuf}\dot{\psi} \end{vmatrix} \tag{22}$$

Using the same procedure we can find:

$$\vec{\sigma}\left(O, S_{ur}/\mathcal{R}_g\right) = \begin{vmatrix} M_{ur}h_{ur}\left(V_{O_y} - l_r\dot{\psi}\right) - I_{xzur}\dot{\psi} \\ -M_{ur}h_{ur}V_{O_x} \\ -M_{ur}l_r\left(V_{O_y} - l_r\dot{\psi}\right) + I_{zur}\dot{\psi} \end{vmatrix} \tag{23}$$

For the sprung mass, the equations are more complicated because of the relationship (12) and because the angular velocity vector is more sophisticated:

$$\vec{\Omega}\left(S_s/\mathcal{R}_c\right) = \dot{\phi}\vec{i}_s + \dot{\theta}\vec{j}_s + \dot{\psi}\vec{k} \tag{24}$$

where $\mathcal{R}_c$ is the vehicle's body frame. With a non-zero lateral acceleration, the pitch axis is inclined. The same remark stands for the roll axis in case of a longitudinal acceleration. The yaw axis remains the same. We then have:

$$\vec{\Omega}\left(S_s/\mathcal{R}_g\right) = \left| \begin{array}{c} \dot{\phi}\cos\theta + \dot{\theta}\sin\phi\sin\theta \\ \dot{\theta}\cos\phi \\ -\dot{\phi}\sin\theta + \dot{\theta}\sin\phi\cos\theta + \dot{\psi} \end{array} \right. \tag{25}$$

The expression of the angular moment in this case is too long, and its derivative (to obtain the dynamic angular moment) is even longer. The same simplifications as in (14) can be applied to moderate the results.

In addition, we should again bring the expressions to the point G:

$$\begin{cases} \vec{\sigma}\left(G, S_s/\mathcal{R}_g\right) = \vec{\sigma}\left(O, S_s/\mathcal{R}_g\right) + M_s\vec{V}\left(O/\mathcal{R}_g\right) \wedge \vec{OG} & (26) \\ \vec{\sigma}\left(G, S_{uf}/\mathcal{R}_g\right) = \vec{\sigma}\left(O, S_{uf}/\mathcal{R}_g\right) + M_{uf}\vec{V}\left(O/\mathcal{R}_g\right) \wedge \vec{OG} & (27) \\ \vec{\sigma}\left(G, S_{ur}/\mathcal{R}_g\right) = \vec{\sigma}\left(O, S_{ur}/\mathcal{R}_g\right) + M_{ur}\vec{V}\left(O/\mathcal{R}_g\right) \wedge \vec{OG} & (28) \end{cases}$$

and using again the torsor properties:

$$\vec{\sigma}\left(G, \Sigma/\mathcal{R}_g\right) = \vec{\sigma}\left(G, S_s/\mathcal{R}_g\right) + \vec{\sigma}\left(G, S_{uf}/\mathcal{R}_g\right) + \vec{\sigma}\left(G, S_{ur}/\mathcal{R}_g\right) \tag{29}$$

Noting I_{i_k} the inertia moment in the direction i of the mass S_k with respect to its CoG, and I_{ij_k} the inertia moment in the plan ij of the mass S_k with respect to its CoG, we obtain the dynamic moment at the point G:

$$\begin{cases} \delta_{G_x} = \ddot{\phi}\left(I_{x_s} + I_{xz_s}\theta + M_s h_s^2\right) + \dot{\phi}\dot{\psi}M_s h_s \phi\left(2h_s\theta - l_s\right) \\ \quad + \ddot{\theta}\phi\left[I_{x_s}\theta - I_{xz_s} + M_s l_s\left(l_s\theta + h_s\right)\right] \\ \quad + \dot{\theta}\dot{\psi}M_s\left[\left(l_s^2 - h_s^2\right) - 4l_s h_s\theta\right] \\ \quad - \ddot{\psi}\left\{I_{xz_s} + I_{xz_{uf}} + I_{xz_{ur}} - M_{uf}h_{uf}l_f + M_{ur}h_{ur}l_r - M_s\left[\left(l_s 2 - h_s^2\right)\theta + l_s h_s\right]\right\} & (30) \\ \delta_{G_y} = \ddot{\theta}\left(I_{y_s} + M_s l_s^2\right) & (31) \\ \delta_{G_z} = -\ddot{\phi}\left[I_{z_s}\theta + I_{xz_s} - M_s h_s\left(l_s - h_s\theta\right)\right] + \ddot{\theta}\phi\left[I_{z_s} - I_{xz_s}\theta + M_s\left(l_s^2 - l_s h_s\theta\right)\right] \\ \quad + 2\dot{\phi}\dot{\psi}M_s h_s\phi\left(l_s\theta + h_s\right) - \dot{\theta}\dot{\psi}M_s\left[2\theta\left(l_s^2 - h_s^2\right) + 2l_s h_s\right] \\ \quad + \ddot{\psi}\left[I_{z_s} + I_{z_{uf}} + I_{z_{ur}} + M_{uf}l_f^2 + M_{ur}l_r^2 + M_s\left(l_s - h_s\theta\right)^2\right] & (32) \end{cases}$$

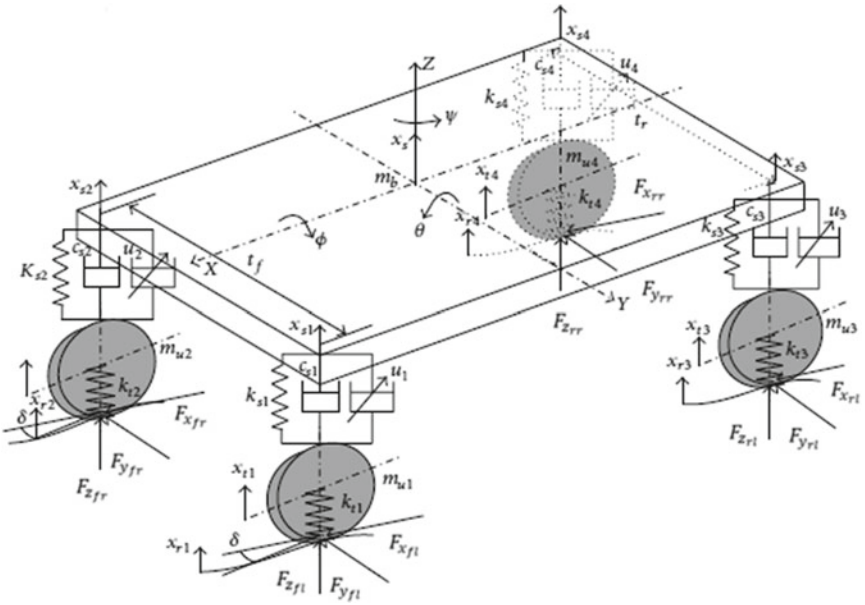

Fig. 3 14-Degrees of Freedom (DoF) vehicle dynamic model (adapted from Zhao & Qu, 2014)

1.3 Exterior Forces Torsor Calculation

This torsor shows the influence of the exterior forces, for example tire forces, on the chosen isolated system. In order to show the influence of the suspensions, we should isolate only the sprung mass where the suspension forces are at the exterior of the studied system. Let us consider Fig. 3.

If we consider the overall system Σ, the exterior forces would be:

- $F_{x_{i,j}}$: $i-j$ longitudinal tire force,[3]
- $F_{y_{i,j}}$: $i-j$ lateral tire force,
- $F_{z_{i,j}}$: $i-j$ vertical tire force,
- $\vec{P}$: the vehicle's weight.

Notice that we do not take into account the aerodynamic forces for example. These forces are not controllable and would be considered as disturbances. They should be rejected by a robust control strategy. Next, we apply the fundamental law of dynamics (3) on the overall system Σ first.

[3] Where "i" is front or rear, and "j" is right or left.

1.3.1 The Dynamic Resultant Theorem

For the linear motion, we apply Eq. (4) using the formulas obtained in Eq. (16):

$$\begin{cases} M\left(\dot{V}_{O_x} - \dot{\psi}V_{O_y}\right) - \ddot{\theta}M_s\left(l_s\theta + h_s\right) - \ddot{\psi}M_s h_s\phi + \dot{\psi}^2 M h_g\theta - 2\dot{\phi}\dot{\psi}M_s h_s \\ \qquad = \left(F_{x_{f,l}} + F_{x_{f,r}}\right)\cos\delta_f + \left(F_{x_{r,l}} + F_{x_{r,r}}\right)\cos\delta_r \\ \qquad - \left(F_{y_{f,l}} + F_{y_{f,r}}\right)\sin\delta_f - \left(F_{y_{r,l}} + F_{y_{r,r}}\right)\sin\delta_r \qquad (33) \\ M\left(\dot{V}_{O_y} + \dot{\psi}V_{O_x}\right) + \ddot{\phi}M_s h_s - \ddot{\psi}M h_g\theta - \dot{\psi}^2 M_s h_s\phi - 2\dot{\theta}\dot{\psi}M_s\left(l_s\theta + h_s\right) \\ \qquad = \left(F_{y_{f,l}} + F_{y_{f,r}}\right)\cos\delta_f + \left(F_{y_{r,l}} + F_{y_{r,r}}\right)\cos\delta_r \qquad (34) \\ \qquad + \left(F_{x_{f,l}} + F_{x_{f,r}}\right)\sin\delta_f + \left(F_{x_{r,l}} + F_{x_{r,r}}\right)\sin\delta_r \\ \ddot{\theta}M_s\left(l_s - h_s\theta\right) - \ddot{\phi}M_s h_s\phi = Mg - F_{z_{f,l}} - F_{z_{f,r}} - F_{z_{r,l}} - F_{z_{r,r}} \qquad (35) \end{cases}$$

with g is the standard gravity acceleration.

1.3.2 The Dynamic Moment Theorem

Let us consider:

- t_f, t_r: the front and rear track of the vehicle respectively,
- h_O: the height of the center of the roll/pitch[4] axis,
- $\sum M_z$: the influence of the self-aligning moments of the tires.

We apply Eq. (5) using the formulas obtained in Eqs. (30)–(32) to calculate the angular motion:

[4] Supposed the same in this chapter for further simplification.

$$\begin{cases} \delta_{G_x} = Mgh_g\phi + \dfrac{t_f}{2}\left(F_{z_{f,l}} - F_{z_{f,r}}\right) + \dfrac{t_r}{2}\left(F_{z_{r,l}} - F_{z_{r,r}}\right) \\ \quad - \left(h_O + h_g\right)\left[\left(F_{y_{f,l}} + F_{y_{f,r}}\right)\cos\delta_f + \left(F_{y_{r,l}} + F_{y_{r,r}}\right)\cos\delta_r\right] \\ \quad - \left(h_O + h_g\right)\left[\left(F_{x_{f,l}} + F_{x_{f,r}}\right)\sin\delta_f + \left(F_{x_{r,l}} + F_{x_{r,r}}\right)\sin\delta_r\right] \end{cases} \tag{36}$$

$$\begin{cases} \delta_{G_y} = Mgh_g\theta + l_f\left(F_{z_{f,l}} + F_{z_{f,r}}\right) - l_r\left(F_{z_{r,l}} + F_{z_{r,r}}\right) \\ \quad + \left(h_O + h_g\right)\left[\left(F_{x_{f,l}} + F_{x_{f,r}}\right)\cos\delta_f + \left(F_{x_{r,l}} + F_{x_{r,r}}\right)\cos\delta_r\right] \\ \quad - \left(h_O + h_g\right)\left[\left(F_{y_{f,l}} + F_{y_{f,r}}\right)\sin\delta_f + \left(F_{y_{r,l}} + F_{y_{r,r}}\right)\sin\delta_r\right] \end{cases} \tag{37}$$

$$\begin{cases} \delta_{G_z} = l_f\left[\left(F_{y_{f,l}} + F_{y_{f,r}}\right)\cos\delta_f + \left(F_{x_{f,l}} + F_{x_{f,r}}\right)\sin\delta_f\right] \\ \quad - l_r\left[\left(F_{y_{r,l}} + F_{y_{r,r}}\right)\cos\delta_r + \left(F_{x_{r,l}} + F_{x_{r,r}}\right)\sin\delta_r\right] \\ \quad + \dfrac{t_f}{2}\left[\left(F_{x_{f,l}} - F_{x_{f,r}}\right)\cos\delta_f - \left(F_{y_{f,l}} - F_{y_{f,r}}\right)\sin\delta_f\right] \\ \quad + \dfrac{t_r}{2}\left[\left(F_{x_{r,l}} - F_{x_{r,r}}\right)\cos\delta_r - \left(F_{y_{r,l}} - F_{y_{r,r}}\right)\sin\delta_r\right] + \sum M_z \end{cases} \tag{38}$$

1.4 The Sprung Mass Dynamics

Regarding roll dynamics, pitch dynamics and the pure vertical dynamics, the vehicle's body should be isolated. This enables the introduction of the suspension forces. In case of active suspensions, as it is the case in Fig. 3, we have (Zhao & Qu, 2014):

$$\begin{cases} F_{s_{f,l}} = k_{s_{f,l}}\left(z_{p_{f,l}} - z_{s_{f,l}}\right) + c_{s_{f,l}}\left(\dot{z}_{p_{f,l}} - \dot{z}_{s_{f,l}}\right) \\ \quad - \dfrac{k_{\phi_f}}{2t_f}\left(\phi - \dfrac{z_{p_{f,l}} - z_{s_{f,l}}}{2t_f}\right) + u_{f,l} \end{cases} \tag{39}$$

$$\begin{cases} F_{s_{f,r}} = k_{s_{f,r}}\left(z_{p_{f,r}} - z_{s_{f,r}}\right) + c_{s_{f,r}}\left(\dot{z}_{p_{f,r}} - \dot{z}_{s_{f,r}}\right) \\ \quad + \dfrac{k_{\phi_f}}{2t_f}\left(\phi - \dfrac{z_{p_{f,r}} - z_{s_{f,r}}}{2t_f}\right) + u_{f,r} \end{cases} \tag{40}$$

$$\begin{cases} F_{s_{r,l}} = k_{s_{r,l}}\left(z_{p_{r,l}} - z_{s_{r,l}}\right) + c_{s_{r,l}}\left(\dot{z}_{p_{r,l}} - \dot{z}_{s_{r,l}}\right) \\ \quad + \dfrac{k_{\phi_r}}{2t_r}\left(\phi - \dfrac{z_{p_{r,l}} - z_{s_{r,l}}}{2t_r}\right) + u_{r,l} \end{cases} \tag{41}$$

$$\begin{cases} F_{s_{r,r}} = k_{s_{r,r}}\left(z_{p_{r,r}} - z_{s_{r,r}}\right) + c_{s_{r,r}}\left(\dot{z}_{p_{r,r}} - \dot{z}_{s_{r,r}}\right) \\ \quad - \dfrac{k_{\phi_r}}{2t_r}\left(\phi - \dfrac{z_{p_{r,r}} - z_{s_{r,r}}}{2t_r}\right) + u_{r,r} \end{cases} \tag{42}$$

where:

- z_{p_i}: vertical travel of tires,
- z_{s_i}: vertical travel of suspensions,
- k_{s_i}: suspension's stiffness,
- c_{s_i}: suspension's damping,
- k_{ϕ_f}, k_{ϕ_r}: the front and rear anti-roll bars stiffness respectively,
- u_{s_i}: control forces of the active suspensions.

Using again the same theorems (4) and (5) and the same simplifications in (14), we can get:

$$\begin{cases} \ddot{\phi}\left(I_{x_s} + I_{xz_s}\theta\right) + \ddot{\theta}\phi\left(I_{x_s}\theta - I_{xz_s}\right) - \ddot{\psi}I_{xz_s} = M_s g h_s \phi \\ \qquad + \dfrac{t_f}{2}\left(F_{s_{f,l}} - F_{s_{f,r}}\right) + \dfrac{t_r}{2}\left(F_{s_{r,l}} - F_{s_{r,r}}\right) \\ \qquad - (h_O + h_s)\left[\left(F_{y_{f,l}} + F_{y_{f,r}}\right)\cos\delta_f + \left(F_{y_{r,l}} + F_{y_{r,r}}\right)\cos\delta_r\right] \\ \qquad - (h_O + h_s)\left[\left(F_{x_{f,l}} + F_{x_{f,r}}\right)\sin\delta_f + \left(F_{x_{r,l}} + F_{x_{r,r}}\right)\sin\delta_r\right] \end{cases} \tag{43}$$

$$\begin{aligned} \ddot{\theta} I_{y_s} &= M_s g h_s \theta + l_f\left(F_{s_{f,l}} + F_{s_{f,r}}\right) - l_r\left(F_{s_{r,l}} + F_{s_{r,r}}\right) \\ &\quad + (h_O + h_s)\left[\left(F_{x_{f,l}} + F_{x_{f,r}}\right)\cos\delta_f + \left(F_{x_{r,l}} + F_{x_{r,r}}\right)\cos\delta_r\right] \\ &\quad - (h_O + h_s)\left[\left(F_{y_{f,l}} + F_{y_{f,r}}\right)\sin\delta_f + \left(F_{y_{r,l}} + F_{y_{r,r}}\right)\sin\delta_r\right] \end{aligned} \tag{44}$$

$$M_s\left[\ddot{\theta}\left(l_s - h_s\theta\right) - \ddot{\phi}h_s\phi\right] = M_s g - F_{s_{f,l}} - F_{s_{f,r}} - F_{s_{r,l}} - F_{s_{r,r}} \tag{45}$$

1.5 Model Simplification and Validation

The vehicle equations of motion developed in this chapter are tedious to implement. Nevertheless, they still can be used for control strategies validation. However, from a control synthesis viewpoint, these equations are inadequate. The models should be simplified enough to deduce control strategies, but not too simple to avoid loosing important information. This is why we have chosen starting from a complex model and then simplify it, rather than doing the inverse and select models such as the bicycle model. This latter for example would be insufficient for simultaneous operation control as braking in a corner for example.

First, we validate the initial vehicle model. To do so, we use as a reference a high-fidelity vehicle model provided by Simcenter Amesim®. Figure 4 illustrates the 15 DoF chassis selected. Complex axle kinematics are used to model the specific joint between the sprung and unsprung masses.

The procedure is simple. We simulate both the high fidelity vehicle model of Amesim® and the model developed previously in several use-cases. We then compare the results of the two models. We identify the order of magnitude of each term in every

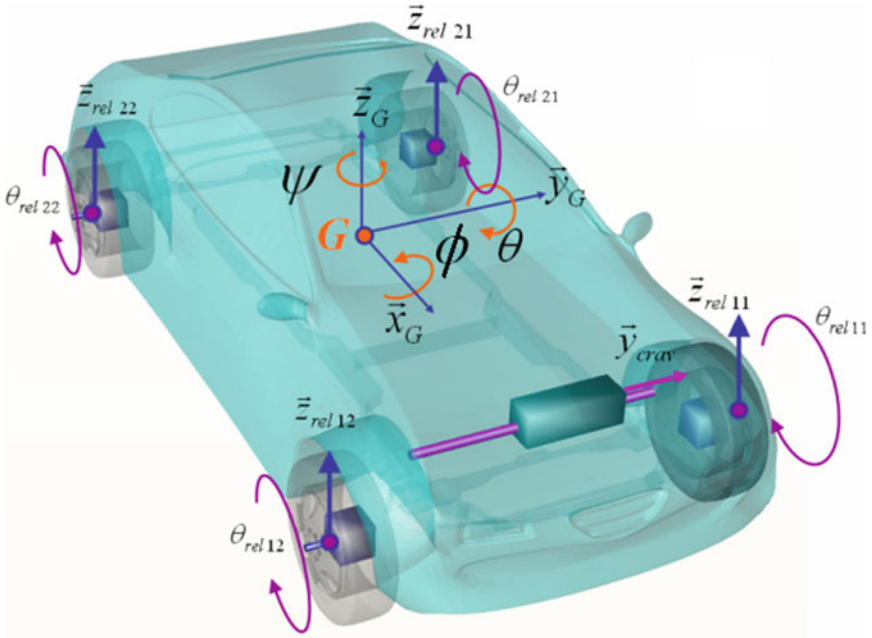

Fig. 4 The 15 DoF chassis provided by Amesim®

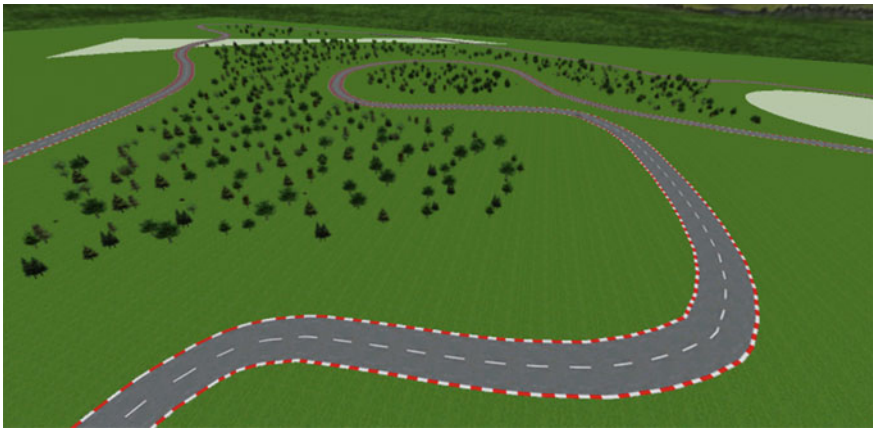

Fig. 5 3D aspect of the Magny-Cours race track with hills area

equation before summing all the components of the equations presented. Then we just simplify the least influencing terms. For a simulation that covers the excitation of all vehicle dynamics, we selected a 3D road reproduced by AmeSim's engineers from a real life race track: the approved International Circuit of Magny-Cours depicted in Fig. 5.

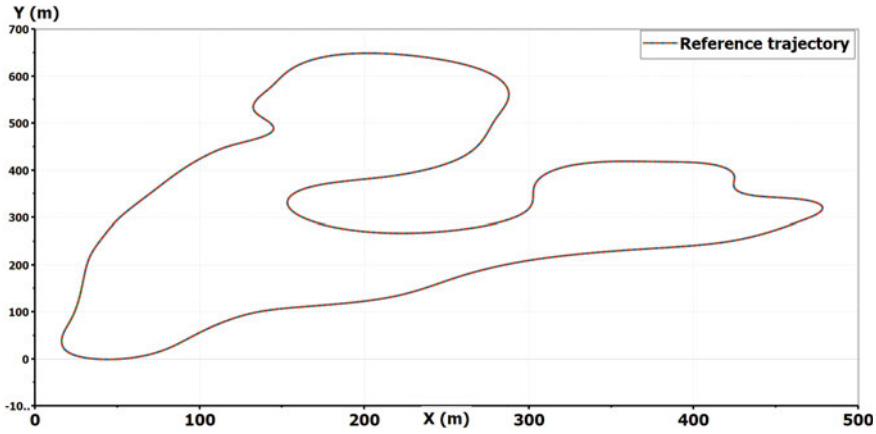

Fig. 6 Magny-Cours trajectory

A top view of the Magny-Cours trajectory is illustrated in Fig. 6.

After the aforementioned simplification procedure, we can obtain the following state-space representation:

$$
\begin{bmatrix}
1 & 0\,0\,0\,0\,0\,0\,0 \\
0 & 1\,0\,0\,0\,0\,0\,0 \\
0 & 0\,1\,0\,0\,0\,0\,0 \\
0 & 0\,0\,1\,0\,0\,0\,0 \\
0 & 0\,0\,0\,1\,0\,0\,0 \\
0 & 0\,0\,0\,0\,1\,0\,0 \\
0 & 0\,0\,0\,0\,0\,1\,0 \\
\dfrac{K_p}{g} + M_s h_s & \\
\dfrac{I_{y_s}}{} & 0\,0\,0\,0\,0\,0\,1 \\
\dfrac{M_s h_s}{I_z}\phi & 0\,0\,0\,0\,0\,0\,1
\end{bmatrix}
\begin{bmatrix}
\dot{V}_x \\ \dot{V}_y \\ V_z \\ \dot{V}_z \\ \dot{\phi} \\ \ddot{\phi} \\ \dot{\theta} \\ \ddot{\theta} \\ \ddot{\psi}
\end{bmatrix}
$$

$$
= \begin{bmatrix}
0\,0\,0\,0 & 0 & 0 & \dfrac{M_s}{M} g & 0 & V_y \\
0\,0\,0\,0 & 0 & 0 & 0 & 0 & -V_x \\
0\,0\,0\,1 & 0 & 0 & 0 & 0 & 0 \\
0\,0\,0\,0 & 0 & 0 & 0 & 0 & 0 \\
0\,0\,0\,0 & 0 & 1 & 0 & 0 & 0 \\
0\,0\,0\,0 & -\dfrac{K_r}{I_{x_s}} & -\dfrac{C_{s_r}}{I_{x_s}} & 0 & 0 & 0 \\
0\,0\,0\,0 & 0 & 0 & 0 & 1 & 0 \\
0\,0\,0\,0 & 0 & 0 & -\dfrac{M - M_s}{M}\dfrac{K_p}{I_{y_s}} & -\dfrac{C_{s_p}}{I_{y_s}} & 0 \\
0\,0\,0\,0 & 0 & 0 & 0 & 0 & 0
\end{bmatrix}
\begin{bmatrix}
V_x \\ V_y \\ z \\ V_z \\ \phi \\ \dot{\phi} \\ \theta \\ \dot{\theta} \\ \dot{\psi}
\end{bmatrix}
\tag{46}
$$

$$
+ \begin{bmatrix}
\dfrac{1}{M} & 0 & 0 & 0 & 0 & 0 \\
0 & \dfrac{1}{M} & 0 & 0 & 0 & 0 \\
0 & 0 & 0 & 0 & 0 & 0 \\
0 & 0 & \dfrac{1}{M} & 0 & 0 & 0 \\
0 & 0 & 0 & 0 & 0 & 0 \\
0 & 0 & 0 & \dfrac{1}{I_{x_s}} & 0 & 0 \\
0 & 0 & 0 & 0 & 0 & 0 \\
0 & 0 & 0 & 0 & \dfrac{1}{I_{y_s}} & 0 \\
0 & 0 & 0 & 0 & 0 & \dfrac{1}{I_z}
\end{bmatrix}
\begin{bmatrix}
F_{x_{tot}} \\ F_{y_{tot}} \\ F_{z_{tot}} \\ M_{x_{tot}} \\ M_{y_{tot}} \\ M_{z_{tot}}
\end{bmatrix}
$$

where:

- z: vertical travel of the sprung mass,
- V_z: vertical velocity of the sprung mass,
- K_r: equivalent overall antiroll bar stiffness,
- C_{s_r}: equivalent overall roll suspension damping,

- K_p: equivalent overall pitch suspension stiffness,
- C_{s_p}: equivalent overall pitch suspension damping,
- I_z: yaw inertia moment of the overall vehicle with respect to its CoG,
- $F_{i_{tot}}$: combination of tire forces projected at the axis "i",
- $M_{i_{tot}}$: combination of moments generated by tire forces with respect to the axis "i".

with:

$$\begin{cases} F_{x_{tot}} = \left(F_{x_{f,l}} + F_{x_{f,r}}\right)\cos\delta_f + \left(F_{x_{r,l}} + F_{x_{r,r}}\right)\cos\delta_r \\ \qquad - \left(F_{y_{f,l}} + F_{y_{f,r}}\right)\sin\delta_f - \left(F_{y_{r,l}} + F_{y_{r,r}}\right)\sin\delta_r & (47) \\ F_{y_{tot}} = \left(F_{y_{f,l}} + F_{y_{f,r}}\right)\cos\delta_f + \left(F_{y_{r,l}} + F_{y_{r,r}}\right)\cos\delta_r \\ \qquad + \left(F_{x_{f,l}} + F_{x_{f,r}}\right)\sin\delta_f + \left(F_{x_{r,l}} + F_{x_{r,r}}\right)\sin\delta_r & (48) \\ F_{z_{tot}} = F_{z_{f,l}} + F_{z_{f,r}} + F_{z_{r,l}} + F_{z_{r,r}} & (49) \\ M_{x_{tot}} = \dfrac{t_f}{2}\left(F_{z_{f,l}} - F_{z_{f,r}}\right) + \dfrac{t_r}{2}\left(F_{z_{r,l}} - F_{z_{r,r}}\right) & (50) \\ M_{y_{tot}} = l_f\left(F_{z_{f,l}} + F_{z_{f,r}}\right) - l_r\left(F_{z_{r,l}} + F_{z_{r,r}}\right) & (51) \\ M_{z_{tot}} = l_f\left[\left(F_{y_{f,l}} + F_{y_{f,r}}\right)\cos\delta_f + \left(F_{x_{f,l}} + F_{x_{f,r}}\right)\sin\delta_f\right] \\ \qquad - l_r\left[\left(F_{y_{r,l}} + F_{y_{r,r}}\right)\cos\delta_r + \left(F_{x_{r,l}} + F_{x_{r,r}}\right)\sin\delta_r\right] \\ \qquad + \dfrac{t_f}{2}\left[\left(F_{x_{f,l}} - F_{x_{f,r}}\right)\cos\delta_f - \left(F_{y_{f,l}} - F_{y_{f,r}}\right)\sin\delta_f\right] \\ \qquad + \dfrac{t_r}{2}\left[\left(F_{x_{r,l}} - F_{x_{r,r}}\right)\cos\delta_r - \left(F_{y_{r,l}} - F_{y_{r,r}}\right)\sin\delta_r\right] + \sum M_z & (52) \end{cases}$$

and:

$$\begin{cases} K_r = K_{\phi_f} + K_{\phi_r} & (53) \\ C_{s_r} = 2c_{s_f}\left(\dfrac{t_f}{2}\right)^2 + 2c_{s_r}\left(\dfrac{t_r}{2}\right)^2 & (54) \\ K_p = 2k_{s_f}l_f^2 + 2k_{s_r}l_r^2 & (55) \\ C_{s_p} = 2c_{s_f}l_f^2 + 2c_{s_r}l_r^2 & (56) \end{cases}$$

where:

- k_{s_f}, k_{s_r}: the front and rear suspension stiffness respectively.[5]
- c_{s_f}, c_{s_r}: the front and rear suspension damping respectively.

By inverting the first matrix, we finally get the state-space representation in the standard form:

[5] The front suspensions are alike by design. The same remark holds for the rear suspensions.

$$
\begin{cases}
\begin{bmatrix} \dot{V}_x \\ \dot{V}_y \\ V_z \\ \dot{V}_z \\ \dot{\phi} \\ \ddot{\phi} \\ \dot{\theta} \\ \ddot{\theta} \\ \ddot{\psi} \end{bmatrix} = \begin{bmatrix} 0\,0\,0\,0 & 0 & 0 & \frac{M_s}{M}g & 0 & V_y \\ 0\,0\,0\,0 & 0 & 0 & 0 & 0 & -V_x \\ 0\,0\,0\,1 & 0 & 0 & 0 & 0 & 0 \\ 0\,0\,0\,0 & 0 & 0 & 0 & 0 & 0 \\ 0\,0\,0\,0 & 0 & 1 & 0 & 0 & 0 \\ 0\,0\,0\,0 & -\frac{K_r}{I_{x_s}} & -\frac{C_{s_r}}{I_{x_s}} & 0 & 0 & 0 \\ 0\,0\,0\,0 & 0 & 0 & 0 & 1 & 0 \\ 0\,0\,0\,0 & 0 & 0 & -\frac{MK_p + M_s^2 h_s g}{MI_{y_s}} & -\frac{C_{s_p}}{I_{y_s}} & 0 \\ 0\,0\,0\,0 & 0 & 0 & -\frac{M_s^2 h_s g}{MI_z}\phi & 0 & 0 \end{bmatrix} \begin{bmatrix} V_x \\ V_y \\ z \\ V_z \\ \phi \\ \dot{\phi} \\ \theta \\ \dot{\theta} \\ \dot{\psi} \end{bmatrix} \\
+ \begin{bmatrix} \frac{1}{M} & 0 & 0 & 0 & 0 & 0 \\ 0 & \frac{1}{M} & 0 & 0 & 0 & 0 \\ 0 & 0 & 0 & 0 & 0 & 0 \\ 0 & 0 & 0 & \frac{1}{I_{x_s}} & 0 & 0 \\ 0 & 0 & 0 & 0 & 0 & 0 \\ -\frac{M_s h_s}{MI_{y_s}} & 0 & 0 & 0 & \frac{1}{I_{y_s}} & 0 \\ -\frac{M_s h_s}{MI_z}\phi & 0 & 0 & 0 & 0 & \frac{1}{I_z} \end{bmatrix} \begin{bmatrix} F_{x_{tot}} \\ F_{y_{tot}} \\ F_{z_{tot}} \\ M_{x_{tot}} \\ M_{y_{tot}} \\ M_{z_{tot}} \end{bmatrix} \qquad (57) \\
\begin{bmatrix} V_x \\ V_y \\ z \\ \phi \\ \theta \\ \dot{\psi} \end{bmatrix} = \begin{bmatrix} 1\,0\,0\,0\,0\,0\,0\,0\,0 \\ 0\,1\,0\,0\,0\,0\,0\,0\,0 \\ 0\,0\,1\,0\,0\,0\,0\,0\,0 \\ 0\,0\,0\,0\,1\,0\,0\,0\,0 \\ 0\,0\,0\,0\,0\,0\,1\,0\,0 \\ 0\,0\,0\,0\,0\,0\,0\,0\,1 \end{bmatrix} \begin{bmatrix} V_x \\ V_y \\ z \\ V_z \\ \phi \\ \dot{\phi} \\ \theta \\ \dot{\theta} \\ \dot{\psi} \end{bmatrix} \qquad (58)
\end{cases}
$$

Regarding the validation procedure, we make use of a driver model provided by Simcenter Amesim® and designed using a Model Predictive Control (MPC) algorithm to track the Magny-Cours path with an adapted velocity profile. Simulations for this severe maneuver are shown in Figs. 7, 8, 9, 10, 11 and 12.

The model shows good precision for all states in severe coupled maneuvers. Note that the effect of slopes is taken into account in this model. This model can then be chosen as a starting model for problems related to Global Chassis Control (GCC) synthesis. It is important to start with a complex full vehicle model and then reduce it while justifying each simplification. Starting with a simplified model, as the bicycle

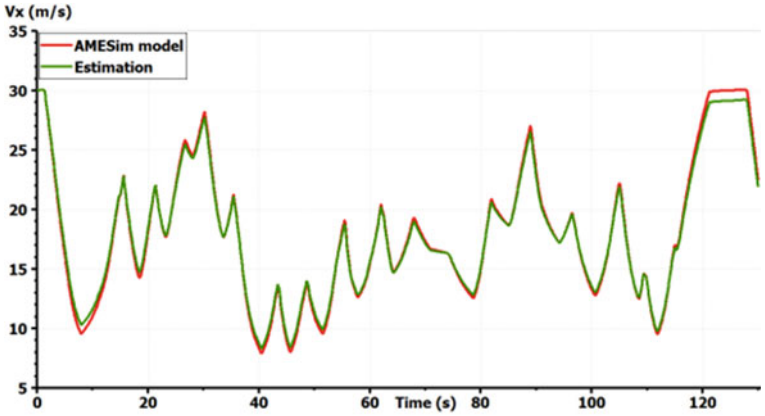

Fig. 7 Vehicle model validation: longitudinal speed

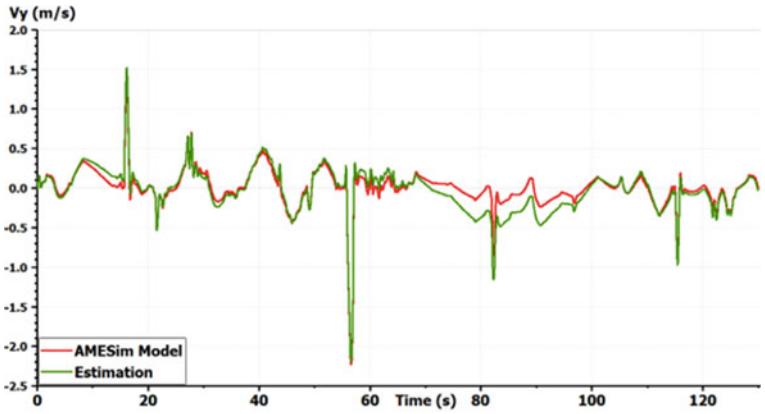

Fig. 8 Vehicle model validation: lateral speed

model, could lead to the ignorance of important dynamics and couplings leading to unexpected emergent behaviors. If only the horizontal motion is concerned, vertical dynamics could be simplified (for the high-level control only) in the control synthesis. However, the vertical forces applied to the tires should always be taken into account as they modify the potential of each tire to drive, brake or steer the vehicle (Pacejka, 2005).

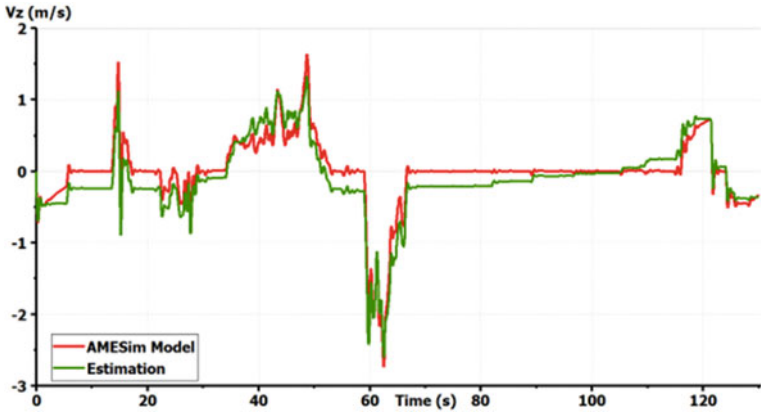

Fig. 9 Vehicle model validation: vertical velocity of the sprung mass

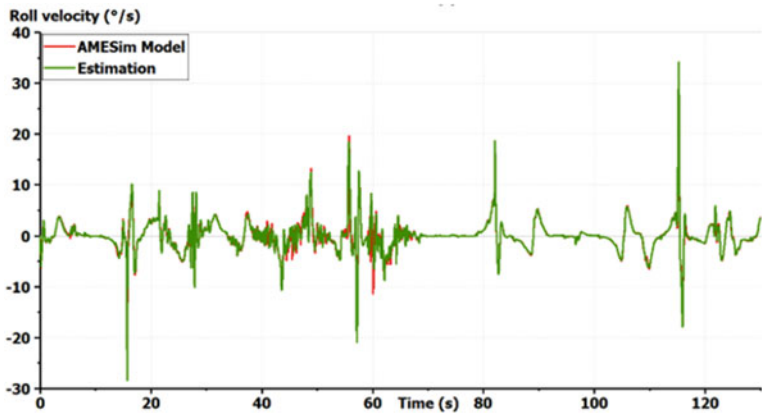

Fig. 10 Validation of the vehicle model: roll velocity

2 Tire Modeling

If the vehicle is equipped at the same time by systems based on lateral tire forces such as the Electric Power Assisted Steering (EPAS) or the 4-Wheel Steering (4WS) system, and others based on longitudinal tire forces such as Anti-lock Braking System (ABS) or the 4-Wheel Driving (4WD) system, the combined slip phenomenon should be taken into account (Pacejka, 2005). From a control synthesis point of view, this requires a tire model giving enough insights to handle coupled operations, for example braking while turning. In this context, the literature is abundant by either empirical models that rely on experimental measures to make simulation more accurate, or complex physical models developed to improve the tire construction by the finite element method. Empirical and semi-empirical models are well-known for their

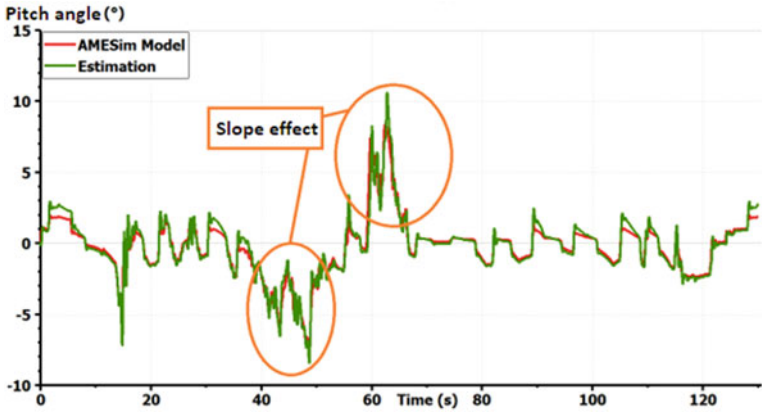

Fig. 11 Vehicle model validation: pitch angle taking into account the slopes

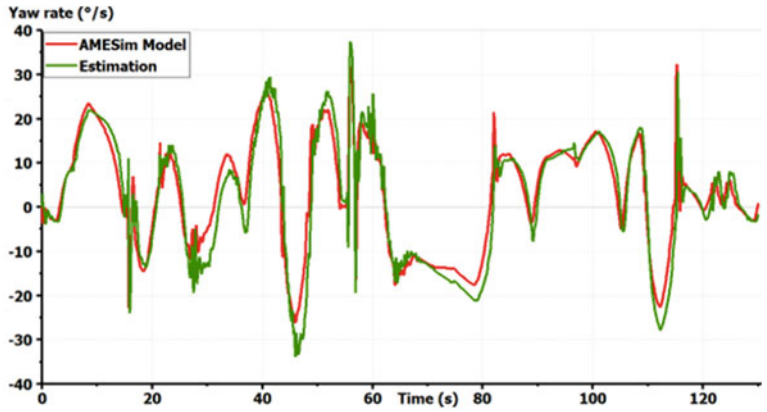

Fig. 12 Vehicle model validation: yaw rate

high-fidelity and accuracy with respect to the reality (Pacejka, 2005), since they are derived from real experiments. However, these models usually depend on identified parameters without much physical significance, which makes them hard to measure or estimate in real-time. This is not suitable for online control problems. Analytic models give a good understanding of tire mechanisms to control the vehicle and foresee its loss of stability. Nonetheless, these models either are not accurate enough for combined slip maneuvers, or they are too complex to be implemented or to use in order to pre-compute a control strategy. We believe that a new tire model especially fitted for GCC should be designed. To do so, we review the most famous tire models that are used in the literature. We compare these models in order to identify the gap that exists with respect to GCC. We will keep our focus on the substantial characteristics that the new tire model should adopt. These characteristics can be summarized as follows:

- The tire model should respect the tire physical fundamentals to give enough insight about the tire behavior. The tire model should be able to depict any perturbation due to tire dynamics and adapt the control strategy. This should not be confused with external disturbances that should be rejected.
- The tire model should describe as precise as possible the combined slip behavior. This is one of the pillars of GCC in combined maneuvers.
- The tire model should be simple enough for controllability issues. The main objective remains developing control algorithms to improve the vehicle motion. The tire model should be easily invertible, and if possible, linear.
- The tire model should depend on a minimum set of parameters that can be measured or estimated in order to favor real-time operations. Also, these parameters should be easily estimated and updated online as fast as possible.

2.1 Tire Physical Fundamentals

In vehicle dynamics, the interface between tires and the road is the one that matters most. We are therefore interested in only the outer layer made of rubber blocks. The rubber is a *viscoelastic* material (Michelin, 2001): the stress is proportional to the deformation (elastic behaviour) and phase-shifted to it (viscous behaviour). To understand this, a closer look into the friction concept is needed. First, we define the tire coordinate system. Same as for the vehicle model, the ISO 8855-2011 depicted in Fig. 13 is adopted:

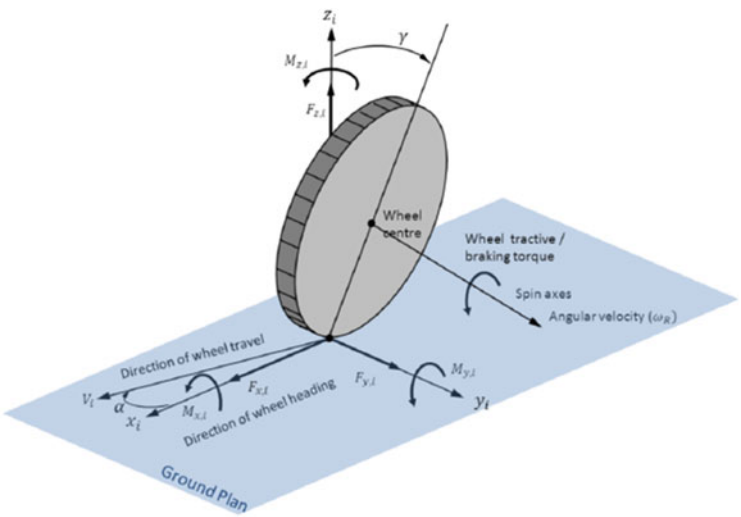

Fig. 13 ISO tire coordinate system